

BED TOPOGRAPHY AND SEDIMENT SORTING IN CHANNEL BEND WITH UNSTEADY FLOW

By Chin-lien Yen,¹ Fellow, ASCE, and Kwan Tun Lee²

ABSTRACT: Bed topography and transverse sediment sorting in an alluvial channel bend were investigated under unsteady-flow conditions with nonuniform sediment. Five experiments, each having the same initial sediment-size gradation but a different inflow hydrograph, were done in a 180° channel bend with a constant radius of curvature. In addition, bed elevations across various sections of the bend were measured, and bed-surface sediment were sampled at the peak and end of the hydrograph in each experiment. Experimental results indicated that the characteristics of the hydrograph have prominent influences on bed topography and transverse sediment sorting. Those cases with a higher ramping rate of the hydrograph have greater deposition heights near the inner bank and larger scour depths near the outer bank. Furthermore, the sediment is finer near the inner bank and coarser near the outer bank in cases with a higher ramping rate. The bed deformation and sediment-size variation correlated well with the unsteady-flow parameter defined in this study. Furthermore, regression relations for transverse bed profile, transverse variation of sediment size, and total amount of sediment discharge were established in terms of the unsteady-flow parameter.

INTRODUCTION

The mechanics of sediment transport in channel bends, frequently appearing in natural rivers, is much more complex than that in straight channels. The complexity is twofold. On one hand, the highly nonuniform sediment in a channel bend is subject not only to longitudinal transport but also to transverse transport and transverse sorting by the secondary flow inherently associated with bends. On the other hand, the unsteadiness of flow in natural rivers certainly has some effects on the structure of the flow field, thereby affecting the motion of sediment particles. The complex phenomena of flow and sediment motion in bends have been studied by many investigators, contributing much to the understanding of this subject. However, many relevant aspects regarding these phenomena require further clarification.

Channel bends with fixed flat beds as well as movable beds have been extensively investigated both theoretically and experimentally. Rozovskii (1957) and Yen (1965) studied the flow characteristics and boundary shear stress distribution in bends with a fixed flat bed. Yen (1967) performed experiments in a channel bend to investigate the equilibrium bed configuration, flow characteristics, and interactions between them. Those studies concerning the transverse bed slope in the fully developed region of a bend, by Engelund (1974), Kikkawa et al. (1976), Falcon and Kennedy (1983), and others, provided a clearer description of flow and bed configuration in river bends under steady-flow conditions. However, the first quantitative model considering nonuniform sediment in bend was proposed by Allen (1970), in which the sediment-size distribution at point bars was reasonably well predicted from the balance of forces exerting on grains placed on idealized empirical bed profiles. Bridge (1976) treated the transverse sorting phenomenon on the basis of Engelund's (1974) transverse bed-slope equation. Odgaard (1982) performed an analysis based on the concept of critical shear stress for sediment motion, and force balance between the transverse bed

shear stress and transverse component of sediment weight, to determine sediment size distribution in transverse direction resulting from lateral sorting. Ikeda et al. (1987) found that sorting of bed material in bends can reduce the maximum equilibrium scour depth as dramatically as 30–40% in the fully developed region. Yen and Lin (1990) conducted four experiments using sediment of different size gradations, demonstrating that sediment-size gradation has a significant influence on bed evolution in channel bends. Since natural river flow is usually unsteady, a great deal of interest in sediment transport under unsteady-flow conditions has arisen within the last two decades. Griffiths and Sutherland (1977) reported sediment discharge variation caused by a translation wave under the conditions of equilibrium as well as nonequilibrium transport. Graf and Suszka (1985) investigated sediment-transport relations under unsteady- and steady-flow conditions in a straight flume. Nouh (1989) also conducted unsteady-flow experiments in a straight flume, finding that initial sediment-size gradation and unsteady-flow characteristics affected the final composition of the armoring layer.

Flow characteristics and sediment motion in channel bends under steady-flow conditions have received much attention. Those investigations concerned with the problem of sediment transport in unsteady flow were all conducted in straight channels. To the writers' knowledge, bed topography and sediment sorting in channel bends under unsteady-flow conditions have never been investigated. In dealing with engineering problems concerning river bends, however, engineers often face an unsteady-flow situation with highly nonuniform sediment. To provide the practicing engineers with better information for planning, design and operation of river engineering projects, some fundamental behaviors of nonuniform sediment in channel bends are investigated in this study under unsteady-flow conditions.

In this study, information regarding bed deformation, sediment-size variation, and sediment discharge is obtained via careful measurements in experiments conducted under different hydrographs. The transverse bed profiles at sections of maximum deformation, the transverse variation of sediment size in the most intensively sorted section and total sediment discharge during the unsteady-flow event are approximated separately by regression equations. The sorting phenomenon in the transverse direction in channel bend is discussed in depth. The writers hope the results reported here can be useful in enhancing the accuracy in predicting bed configuration and bed-surface sediment size in channel bends

¹Prof., Dept. of Civ. Engrg./Sr. Res. Fellow, Hydr. Res. Lab., Nat. Taiwan Univ., Taipei, Taiwan 10617.

²Assoc. Prof., Dept. of River and Harbor Engrg., Nat. Taiwan Oc. Univ.; formerly, Post-doctoral Res. Assoc., Hydr. Res. Lab., Nat. Taiwan Univ., Taipei, Taiwan 20204.

Note. Discussion open until January 1, 1996. To extend the closing date one month, a written request must be filed with the ASCE Manager of Journals. The manuscript for this paper was submitted for review and possible publication on January 28, 1994. This paper is part of the *Journal of Hydraulic Engineering*, Vol. 121, No. 8, August, 1995. ©ASCE, ISSN 0733-9429/95/0008-0591-0599/\$2.00 + \$.25 per page. Paper No. 7755.

under unsteady-flow conditions as well as in shedding additional insight into the physical process of river meandering.

THEORETICAL CONSIDERATIONS

Unsteady-Flow Effect

The pattern of scour and deposition in a channel bend is dependent on the longitudinal and transverse flows. The transverse flow causes the sediment motion on bed surface to deviate from the general longitudinal direction (s -direction) of the flow. The deviation angle may be expressed as (Ho 1987)

$$\delta_i = \tan^{-1} \left(\frac{\tau_{on} + \frac{2}{3} \frac{\beta g}{\alpha \lambda} d_i \sin \theta_n}{\tau_{os} + \frac{2}{3} \frac{\beta g}{\alpha \lambda} d_i \sin \theta_s} \right) \quad (1)$$

in which δ_i = deviation angle; τ_{on} and τ_{os} = n - and s -components of the bed shear stress, respectively (the n -direction is the transverse direction normal to the s -direction and positive toward the concave bank); $\beta = (\rho_s - \rho)/\rho$; ρ and ρ_s = water and sediment densities, respectively; g = gravitational acceleration; d_i = mean diameter of the i th size fraction; α and λ = shape factor and sheltering coefficient of sediment, respectively; and θ_s and θ_n = longitudinal and transverse bed slope angles, respectively. Eq. (1) indicates that the deviation angle depends on the components of bed shear stress, the evolving bed slopes, and the size of sediment particle.

On the basis of experimental results (Yen 1965, 1967), the ratio of bed shear components, τ_{on}/τ_{os} , obviously varies with flow depth, bed topography, and point position on bed surface in a nonuniform bend with steady flow. Therefore, it can be generally written as

$$\frac{\tau_{on}}{\tau_{os}} = f \left(\frac{h}{r}, \theta, \frac{\Delta Z_b}{h} \right) \quad (2)$$

where r and θ = radial and angular coordinates of the bend; h = flow depth; and ΔZ_b = bed deformation. In the case of a uniform bend flow with no bed deformation, τ_{on}/τ_{os} is a function only of h/r for a given bend. Zimmermann and Kennedy (1978) and Falcon and Kennedy (1983) have shown that for a uniform bend flow $\tau_{on}/\tau_{os} = b_{ns}(h/r)$, where b_{ns} is dependent on resistance coefficient. This relation for uniform bend flow clearly indicates that the flow depth has a prominent influence on τ_{on}/τ_{os} . One may therefore infer that the flow depth also has a significant influence on τ_{on}/τ_{os} in a nonuniform bend flow. However, this relation may not be accurate for use in nonuniform bend flow.

Under unsteady-flow conditions, both the flow depth and bed deformation change as the discharge changes with time, thereby producing different patterns of flow and resulting in a variation of τ_{on}/τ_{os} with respect to time. Therefore, the deviation angle of a sediment particle moving on the bed surface in the bend, as expressed by (1), and consequently the pattern of sediment motion can be expected to continuously vary throughout the entire duration of a hydrograph. Thus, the phenomena brought by unsteady flow will have some effects on the formation of bed topography and the variation of sediment size in the transverse direction. Therefore, results obtained from previous studies based on steady-flow conditions may not be sufficiently accurate in describing the bed topography and the variation of sediment size in channel bend with unsteady flow.

Dimensionless Parameters

In this study, the dependent variables to be considered are the bed deformation ΔZ_b , surface sediment median diameter

d , and the geometric standard deviation of sediment size gradation $\sigma (= \sqrt{d_{84.1}/d_{15.9}})$ at any given location. Here, $d_{84.1}$ is the grain size of 84.1% finer and $d_{15.9}$ is the grain size of 15.9% finer. The independent variables include five groups: channel geometries, fluid properties, sediment properties, flow characteristics, and time. Channel geometries, fluid properties, and sediment properties are fixed in the experiments; in addition, Reynolds numbers are sufficiently large and Froude numbers sufficiently small for their influences to be negligible. Under these conditions, the following functional relationship can be obtained (Lee 1991):

$$\frac{\Delta Z_b}{h_o}, \frac{d}{d_o}, \frac{\sigma}{\sigma_o} = F_{1,2,3} \left(\frac{r}{r_c}, \theta, W_t, P \right) \quad (3)$$

where r and θ = radial and angular coordinates of the bend, respectively; $W_t = u_{*o}^2 \nabla / (gh_o^3 B)$; $P = (h_p - h_o) / (t_d u_{*o})$; r_c = centerline radius of the bend; B = channel width; h_o = initial flow depth (base flow) at the upstream end; h_p = flow depth at the peak of hydrograph at the upstream end; u_{*o} = shear velocity of the base flow at the upstream end; ∇ = total volume of water under the hydrograph (excluding the base flow); d_o = initial median size of sediment; σ_o = initial geometric standard deviation of sediment size gradation; and t_d = duration of hydrograph.

When the base flow is set equal to the condition for incipient motion of median sediment size, and if the energy slope is assumed to remain nearly the same during the entire duration of the hydrograph, W_t can be considered an index of total flow work done on the bed. W_t is relevant to transport of sediment in the entire hydrograph duration.

To gain better insight into parameter P , the hydrograph can be considered a series of flows with different discharges (excluding base flow). The duration of each discharge is a function of the ramping rate of the hydrograph. For each discharge, the bed deformation is dependent on the discharge and its duration. The total deformation, i.e., the summation of the incremental deformations generated by the series of flows, is a function of the total volume ∇ and ramping rate of the hydrograph. If ∇ and the base flow are fixed, the total deformation is dependent only on the ramping rate. Therefore, P characterizes the flow unsteadiness in this study.

To show the effect of flow unsteadiness, the hydrographs selected for the experiments are such that W_t is the same for all the five runs. Therefore, (3) is reduced to

$$\frac{\Delta Z_b}{h_o}, \frac{d}{d_o}, \frac{\sigma}{\sigma_o} = F_{4,5,6} \left(\frac{r}{r_c}, \theta, P \right) \quad (4)$$

Eq. (4) is used as a guide for conducting laboratory experiments and analyzing the results from the experiments.

EXPERIMENTS

Facilities and Procedures

Experiments were conducted in a laboratory channel bend having a central angle of 180° , $r_c = 4$ m and $B = 1$ m. The bend is connected with a stilling basin, an upstream straight reach of 11.5 m, a downstream straight reach of the same length, and a sediment settling tank. The water depth was controlled by a weir at the downstream end, which was so positioned as to produce roughly a uniform flow along the bend with the base flow discharge. Each cross section of the bend is identified by its respective angular position. In the upstream straight reach, it is identified by the distance from the beginning of the bend (negative), and in the downstream one by the distance from the end of the bend (positive), respectively. A layer of sand around 20 cm thick, with $d_o = 1.0$ mm and $\sigma_o = 2.5$, was placed on the bed before each run

of experiment began. Sand was first sieved into eight sizes, then used to compose a desired size gradation. The graded sediment was so carefully laid onto the bed as to avoid mechanical segregation. The channel was equipped with two rails on which an instrument carriage was mounted. The rails served as the reference line that was adjusted to have a slope of 0.002. The sand bed surface was smoothed by a plate attached to the instrument carriage to skim the uneven top layer off the bed surface so as to have the same slope as the rails. Next, the sand bed was very slowly filled with water through the downstream end so as to prevent hydraulic segregation. After the water level is raised to a depth equivalent to that of the base flow, the flow was started to run at the desired discharge. No sediment was supplied from upstream.

The base flow was set at $0.02 \text{ m}^3/\text{s}$ ($h_o = 5.44 \text{ cm}$, $u_{*o} = 0.031 \text{ m/s}$), determined according to the condition of incipient motion for the sediment with $d_o = 1.0 \text{ mm}$. To avoid the presence of undesirable cross wave at the downstream part of the bend, the maximum peak discharge of the hydrographs adopted was limited to $0.075 \text{ m}^3/\text{s}$. The peak of the hydrograph employed in the present experiment was set at the point of the first third of its duration. Also, W_i is maintained constant for all the hydrographs employed. Information for the hydrographs is provided in Fig. 1 and Table 1. The discharge was controlled manually by a sluice gate, whose opening was adjusted at a step of 1 mm each time. Measurements of water levels taken by point gauge at the upstream end indicated that the error of discharge was within $\pm 0.5\%$ of the prescribed values.

Measurements of bed elevation, also taken by point gauge, were made at the peak and the end of hydrograph for each run of experiments after the flow was stopped and the water was completely but slowly drained. Next, the sediment settling tank was lifted for sampling and the sediment accumulated during the period was weighed. For each cross section, sampling of the surface bed layer was conducted at six locations. The sampling technique used by Little and Mayer (1972) and Yen and Lin (1990) was employed for the exper-

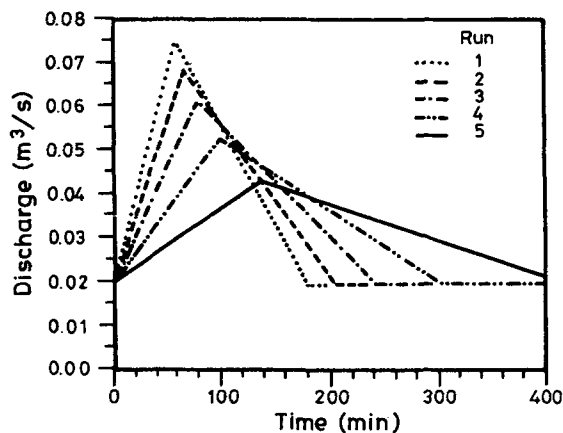


FIG. 1. Hydrographs for Experiments

TABLE 1. Characteristics of Hydrographs Employed

Run (1)	Peak flow Q_p (m^3/s) (2)	Peak flow depth h_p (m) (3)	Duration t_d (min) (4)	Unsteady flow parameter P (10^{-4}) (5)
1	0.0750	0.129	180	2.21
2	0.0685	0.121	204	1.76
3	0.0613	0.113	240	1.31
4	0.0530	0.103	300	0.86
5	0.0436	0.091	420	0.46

iments in this study. Melted wax was poured into a rectangular area (15 cm by 20 cm) enclosed by hemp ropes. Then the solidified wax sheet with sediment adhered to it was carefully removed and placed in hot water to separate the sediment particles from the wax. The sediment was then dried, weighed, and sieved for size gradation. Further details of this procedure are provided in Lee (1991).

Presentation of Data

Contours of bed topography at the end of each of the five experimental runs are separately shown in Figs. 2(a)–2(e). The numerals on the contours are $\Delta Z_b/h_o$ values. The max-

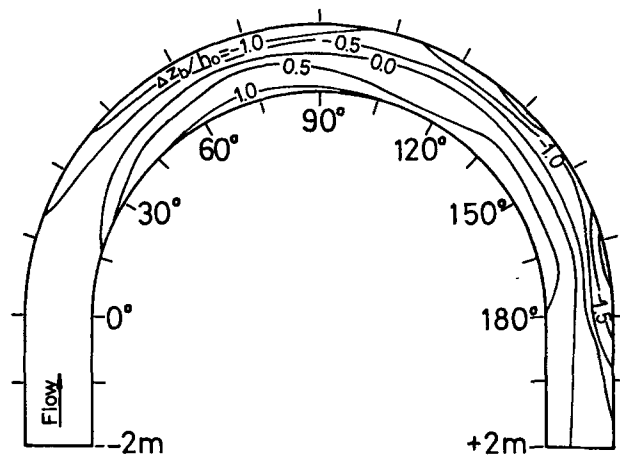


FIG. 2(a). Contours of Bed Deformation for Run 1

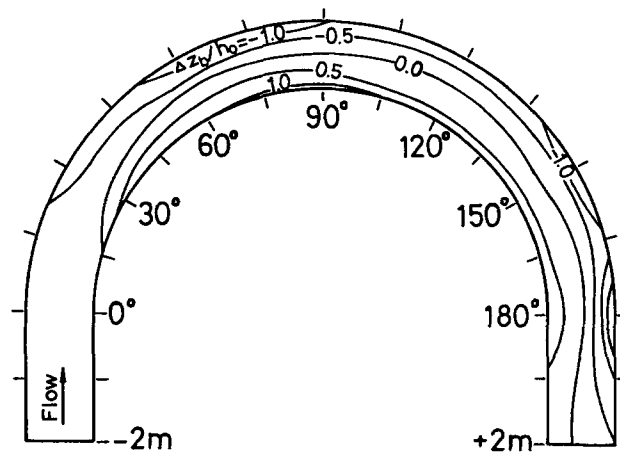


FIG. 2(b). Contours of Bed Deformation for Run 2

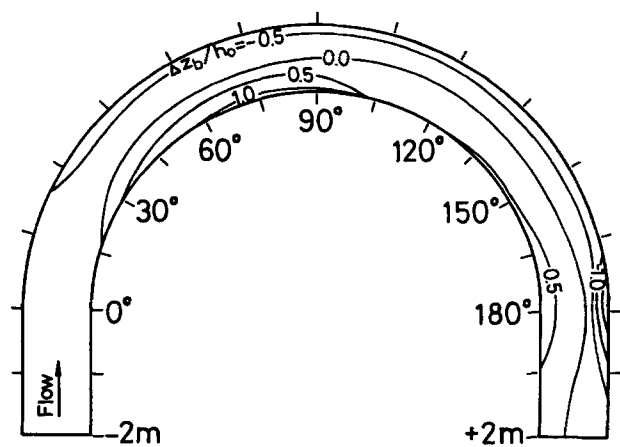


FIG. 2(c). Contours of Bed Deformation for Run 3

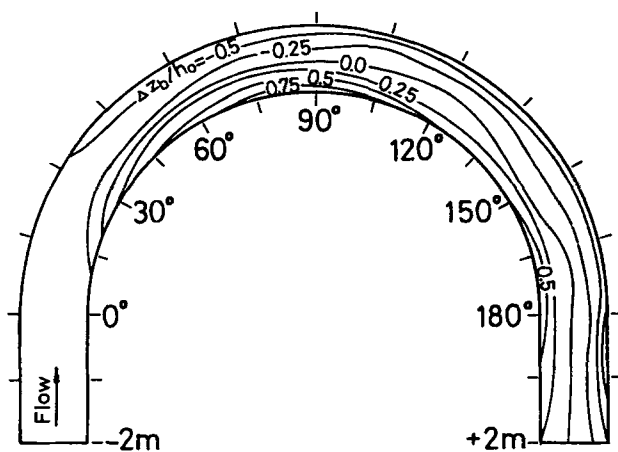


FIG. 2(d). Contours of Bed Deformation for Run 4

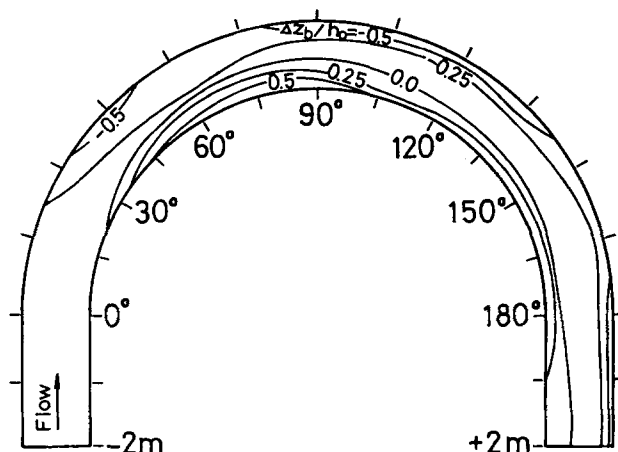


FIG. 2(e). Contours of Bed Deformation for Run 5

imum deposition of all ($\Delta Z_b/h_o = 1.13$) occurred near the inner bank at section 75° at the end of run 1 (see Table 2). Furthermore, the maximum scour of all ($\Delta Z_b/h_o = -2.06$) took place near the outer bank at section 165° also at the end of the same run (see Table 3). The area of maximum scour shifts somewhat downstream as the parameter P decreases [see Figs. 2(a)–2(e)]. At the section of maximum scour, the transverse bed slope is 0.176 in run 1 and it decreases to 0.045 in run 5.

The contours of d/d_o are shown in Figs. 3(a)–3(e). Experimental results reveal that the largest variation of d/d_o in the transverse direction occurred near section 90° in all five runs, indicating that the most intensive transverse sorting is in this area. The maximum d/d_o value of all is 3.60 in run 1 and the minimum is 0.63, also in run 1 (see Table 4). The total amounts of sediment collected in the settling tank at the peak and the end of hydrograph are listed in Table 5. Their respective d/d_o and σ/σ_o values are also presented in the same table, which reveals that the total weight of sediment collected increases as P increases. The d/d_o and σ/σ_o values are all less than or

equal to 1.0, and σ/σ_o generally decreases as P decreases (see Table 5).

RESULTS

Bed Configuration

The contours in Figs. 2(a)–2(e) and the longitudinal bed profiles in Fig. 4 clearly indicate the presence of a scour region for $r/r_c > 1.0$ and a deposition region for $r/r_c < 1.0$. Appreciable bed scour and deposition begin at about section 30° and gradually reduce after section 180°. Apparently, the bed topographies are quite different among the five runs of experiments. The difference can be attributed to the effect of the unsteady flow parameter, as indicated in (4). A close examination of the bed topographies and the longitudinal profiles reveals that the area of maximum deposition height is located between sections 75° and 90°; in addition, the area of maximum scour depth is between sections 165° and 180°. The transverse bed profiles in these two areas should be of great interest to practicing engineers. The transverse bed profiles for the sections of maximum deposition are shown in Fig. 5 and Table 2. The profiles for the sections of maximum scour are shown in Fig. 6 and Table 3. These figures and tables indicate that those cases with higher P values (runs 1 and 2) have greater deposition heights near the inner bank and larger scour depths near the outer bank. Figs. 5 and 6 also reveal that the point of no change in bed elevation (i.e., $\Delta Z_b/h_o = 0$) generally shifts toward the outer bank as P increases. Furthermore, the difference in bed elevation between the outer and inner banks increases with an increasing P value. The transverse bed profiles shown in Figs. 5 and 6 have a general shape similar to the negative hyperbolic tangent function. Therefore, this particular function is employed in the regression equation for the transverse bed profile as follows:

$$\frac{\Delta Z_b}{h_o} = -a_1 \tanh \left[10 \left(\frac{r}{r_c} - b_1 \right) \right] - c_1 \quad (5)$$

in which a_1 , b_1 , and c_1 = coefficients. The coefficient a_1 is a condition imposed on the hyperbolic tangent function so that it can adequately fit the difference in bed elevation between the inner and outer banks. The coefficient b_1 is a quantity associated with the transverse location of the point where $\Delta Z_b/h_o = 0$; in addition, the coefficient c_1 is a quantity associated with the vertical location of the point of inflection of the function. The values for a_1 , b_1 , and c_1 evaluated from the bed profiles shown in Figs. 5 and 6 are plotted in Fig. 7 as a function of the unsteady-flow parameter $P_1 (= P \times 10^4)$. Regression analyses performed on the data for each coefficient yield the following:

$$a_1 = a_{11} + \frac{a_{12}}{1 + \exp[-a_{13}(P_1 - a_{14})]} \quad (6a)$$

$$b_1 = b_{11} + b_{12}P_1 \quad (6b)$$

TABLE 2. Transverse Variation of $\Delta Z_b/h_o$ at Section of Maximum Deposition

Run (1)	Section (2)	r/r_c										
		0.900 (3)	0.913 (4)	0.925 (5)	0.950 (6)	0.975 (7)	1.000 (8)	1.025 (9)	1.050 (10)	1.075 (11)	1.088 (12)	1.100 (13)
1	75°	1.13	1.03	0.99	0.86	0.75	0.55	0.30	-0.50	-1.25	-1.47	-1.54
2	75°	0.92	0.81	0.70	0.57	0.35	0.03	-0.11	-0.33	-0.79	-0.88	-1.00
3	75°	0.88	0.81	0.74	0.53	0.30	-0.06	-0.18	-0.24	-0.47	-0.57	-0.65
4	90°	0.81	0.74	0.65	0.33	0.17	-0.07	-0.11	-0.29	-0.33	-0.44	-0.58
5	90°	0.75	0.72	0.63	0.29	-0.02	-0.07	-0.07	-0.13	-0.42	-0.42	-0.40

TABLE 3. Transverse Variation of $\Delta Z_b/h_o$ at Section of Maximum Scour

Run (1)	Section (2)	r/r_c										
		0.900 (3)	0.913 (4)	0.925 (5)	0.950 (6)	0.975 (7)	1.000 (8)	1.025 (9)	1.050 (10)	1.075 (11)	1.088 (12)	1.100 (13)
1	165°	0.86	0.80	0.73	0.53	0.37	0.29	0.06	-0.66	-1.34	-1.77	-2.06
2	180°	0.83	0.66	0.61	0.51	0.28	0.16	-0.03	-0.35	-1.04	-1.43	-1.62
3	180°	0.82	0.69	0.62	0.40	0.28	0.07	-0.21	-0.66	-0.96	-1.39	-1.55
4	180°	0.52	0.40	0.36	0.13	0.04	-0.07	-0.14	-0.19	-0.33	-0.60	-0.67
5	180°	0.32	0.18	0.08	-0.03	-0.09	-0.08	-0.07	-0.18	-0.24	-0.35	-0.42

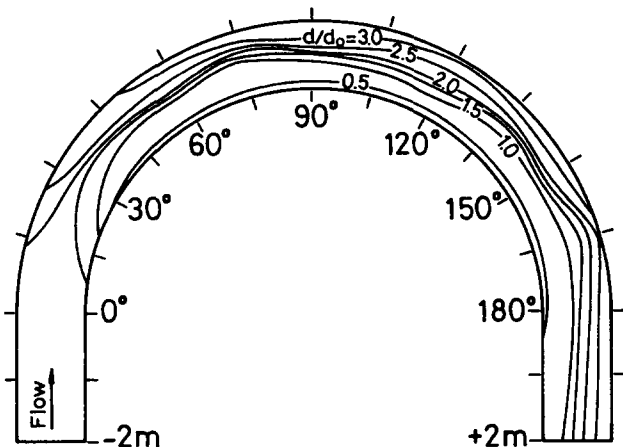


FIG. 3(a). Contours of Median Sediment Size for Run 1

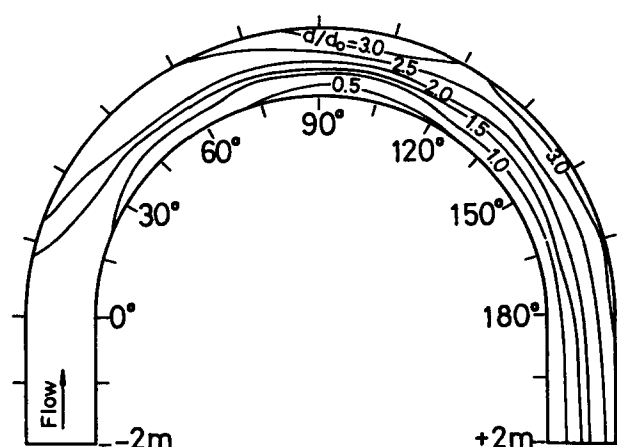


FIG. 3(d). Contours of Median Sediment Size for Run 4

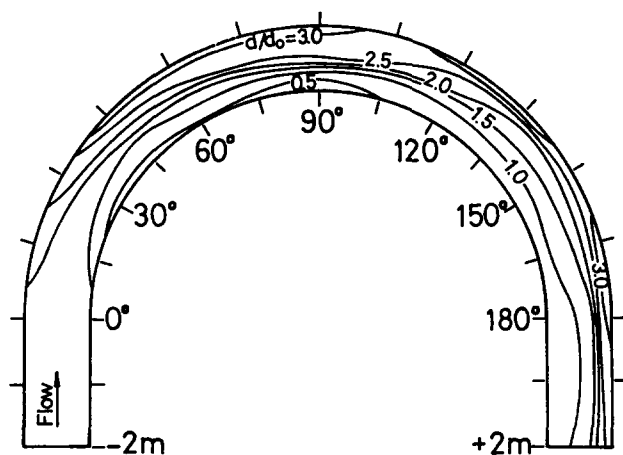


FIG. 3(b). Contours of Median Sediment Size for Run 2

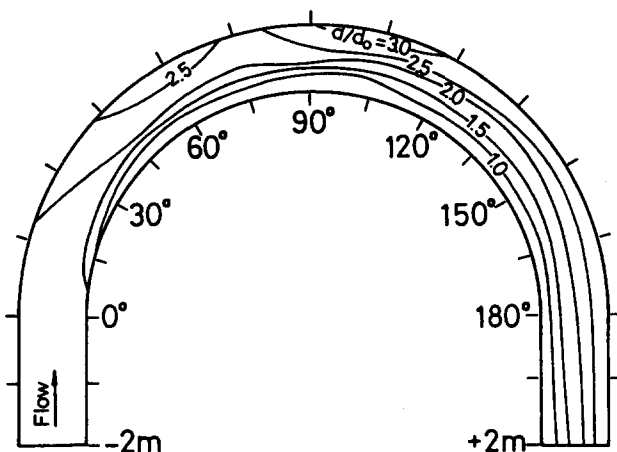


FIG. 3(e). Contours of Median Sediment Size for Run 5

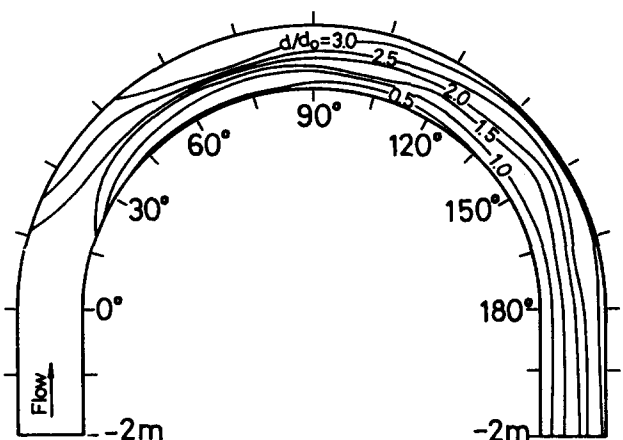


FIG. 3(c). Contours of Median Sediment Size for Run 3

TABLE 4. Transverse Variation of d/d_o at Section 90°

Run (1)	r/r_c					
	0.906 (2)	0.944 (3)	0.981 (4)	1.019 (5)	1.056 (6)	1.094 (7)
1	0.63	0.80 ^a	1.30 ^a	2.58	2.89	3.60
2	0.64	0.95 ^a	2.04	2.52	3.00	3.48
3	0.66	1.00 ^a	2.00 ^a	2.24	2.88	3.29
4	0.70	1.00 ^a	2.25	2.16	2.70	2.89
5	0.70	1.05	2.15	2.48	2.41	2.73

^aCorrected by using information from Fig. 3.

$$c_1 = c_{11} + \frac{c_{12}}{1 + \exp[-c_{13}(P_1 - c_{14})]} \quad (6c)$$

where a_{11} , a_{12} , a_{13} , a_{14} , b_{11} , b_{12} , c_{11} , c_{12} , c_{13} , and c_{14} = coefficients as provided in Table 6. These regression equations are plotted in Figs. 7(a) and 7(b) for sections of maximum deposition and those of maximum scour, respectively. The data points at $P_1 = 0$ shown in Figs. 7(a) and 7(b) are obtained

TABLE 5. Amounts of Sediment Collected and Their Properties during Hydrograph

Run (1)	P (2)	Sediment Collected ^a			d/d_o		σ/σ_o	
		W_{sr} (kg) (3)	W_{sf} (kg) (4)	W_s (kg) (5)	Peak (6)	End (7)	Peak (8)	End (9)
1	2.21	81.09	136.50	217.59	0.96	1.00	0.88	0.90
2	1.76	52.62	68.38	121.00	0.92	0.95	0.85	0.82
3	1.31	34.34	40.85	75.19	0.96	0.90	0.81	0.77
4	0.86	22.29	31.66	53.95	0.95	0.96	0.72	0.80
5	0.46	21.22	17.77	38.99	0.74	0.73	0.76	0.78

^a W_{sr} = amount collected for the rising limb; W_{sf} = amount collected for the falling limb; $W_s = W_{sr} + W_{sf}$.

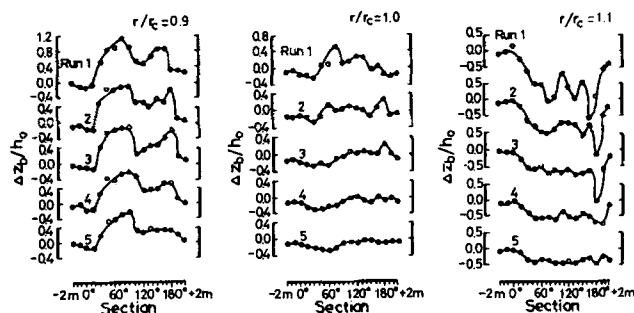


FIG. 4. Longitudinal Bed Profiles

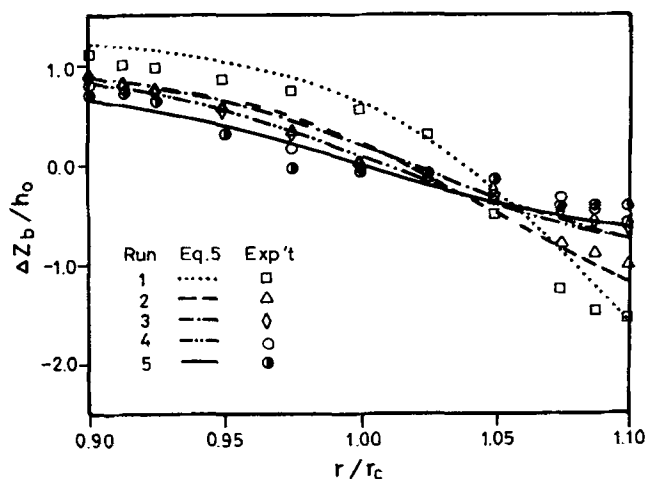


FIG. 5. Transverse Bed Profiles at Section of Maximum Deposition

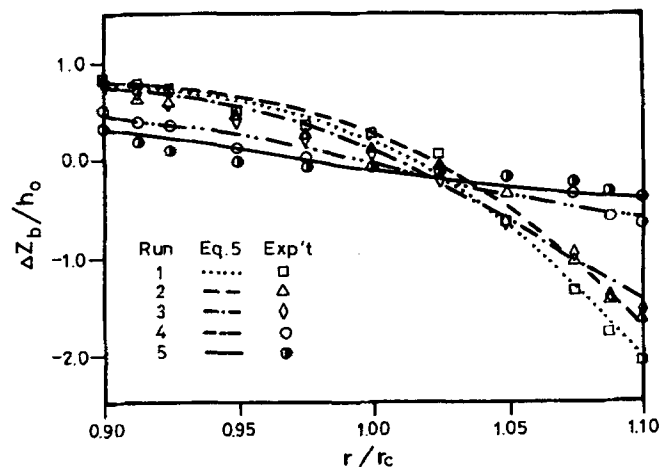


FIG. 6. Transverse Bed Profiles at Section of Maximum Scour

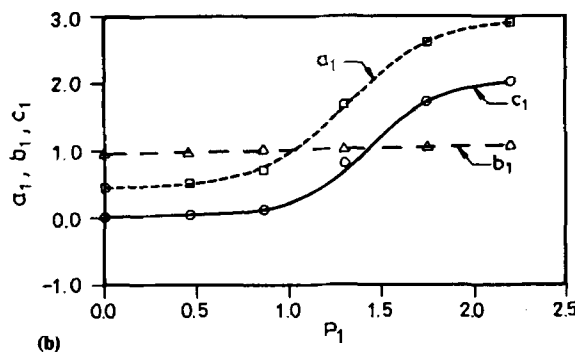
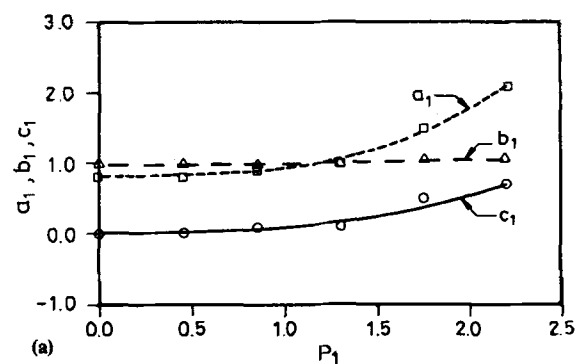


FIG. 7. Coefficients a_1 , b_1 , and c_1 as Functions of P_1 : (a) Section of Maximum Deposition; (b) Section of Maximum Scour

TABLE 6. Coefficients for Eq. (6)

Coefficient (1)	Section	
	Maximum deposition (2)	Maximum scour (3)
a_{11}	0.80	0.45
a_{12}	3.65	2.52
a_{13}	2.31	4.23
a_{14}	2.32	1.32
b_{11}	0.96	0.97
b_{12}	0.04	0.06
c_{11}	0.00	0.03
c_{12}	1.95	2.03
c_{13}	2.01	5.18
c_{14}	2.48	1.43

from a well-calibrated numerical simulation model for steady flow (Yen and Lee 1991). They are not included in the regression analysis, but are shown there for comparison. This comparison indicates that (6a)–(6c) behave reasonably well. Careful examination of the contours in Figs. 2(a)–2(e) reveals that the bed topography varies along the longitudinal direction to some extent—even in the lower half of the bend. Strictly speaking, no fully developed flow is present in the bend in the range of the current experiments. Therefore, coefficients a_1 , b_1 , and c_1 can be expected to vary with θ . Efforts have been made in this study to evaluate the variations of these coefficients with θ . However, the dependence of the coefficients on θ is secondary, except for the first quarter of the bend, and it is not in a very systematic way. Therefore, no further discussion concerning this particular aspect is provided here.

Bed-Surface Sediment

Figs. 3(a)–3(e) indicate that the transverse sorting phenomenon becomes clearly visible beginning at around section 15° and continues through section 180°. After the flow leaves the bend, the transverse sorting phenomenon gradually reduces as the secondary current decays. Furthermore, d/d_o ,

values near the outer bank in the runs with higher P are larger than those in the runs with lower P . On the other hand, the d/d_o value near the inner bank increases with a decreasing P . This variation of d/d_o is also shown in Table 4 as a function of P . This phenomenon can be accounted for by the fact that the runs with higher P values have larger scour depths near the outer bank and larger deposition heights near the inner bank. This results in larger transverse bed slope and therefore relatively larger transverse component of gravity for a larger particle to act against the transverse component of bed shear stress. Consequently, only very fine particles are finally transported to the inner bank region as the transverse bed slope becomes greater.

The transverse variations of d/d_o for section 90° are plotted in Fig. 8. They also exhibit a general shape of the positive hyperbolic tangent function and are therefore approximated by the following regression equation:

$$\frac{d}{d_o} = a_2 \tanh \left[10 \left(\frac{r}{r_c} - b_2 \right) \right] + c_2 \quad (7)$$

in which a_2 , b_2 , and c_2 = coefficients. The values of a_2 , b_2 , and c_2 are evaluated from experimental data. These coefficients also vary with P . A regression equation for each coefficient is obtained as a function of P_1 and given as follows:

$$a_2 = 1.77 + 0.295P_1 \quad (8a)$$

$$b_2 = 0.93 + 0.016P_1 \quad (8b)$$

$$c_2 = 0.85 + 0.296P_1 \quad (8c)$$

These regression equations are plotted in Fig. 9 together with the data evaluated from the experimental results.

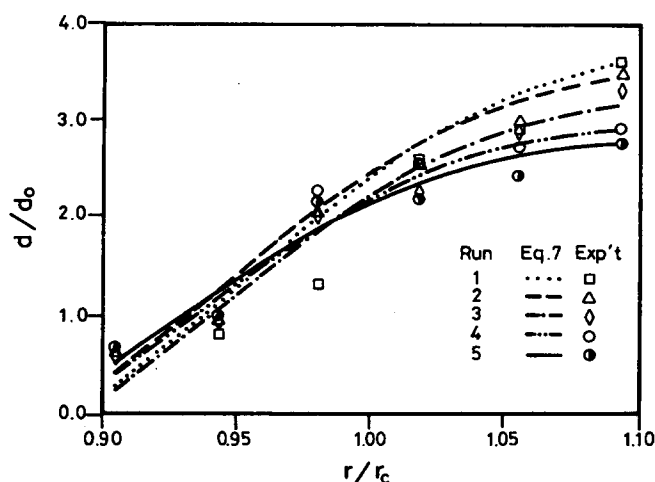


FIG. 8. Transverse Variation of Sediment Size at Section 90°

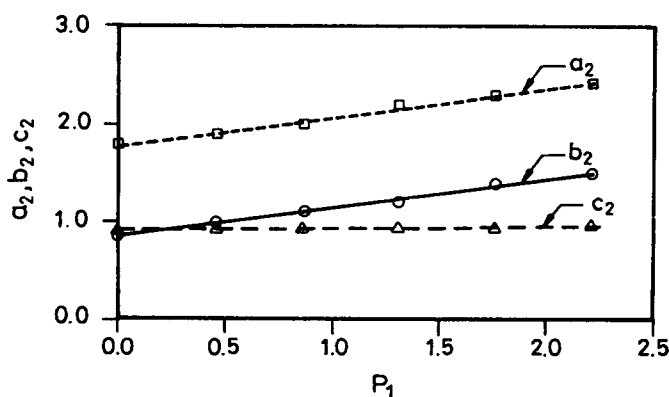


FIG. 9. Coefficients a_2 , b_2 , and c_2 as Functions of P_1

In the outer-bank region, the high longitudinal velocity and the intensive transverse sorting reduce the hiding effect of the nonuniform sediment. The proportion of the fine sediment remaining on the bed surface in this region is therefore substantially less than that in the straight reach, as found in Fig. 10, for example, in which the sediment-size gradation curve for the outer-bank region at section 90° has a quite large shift to the right of that at 4 m upstream from the bend entrance. However, the transverse sorting reduces somewhat after section 90° due to the reduction of shear stress in the separation zone of the scour hole. Therefore, the sediment-size gradation curves for sections 135° and 180° shift to the left of that for section 90°, as also observed in Fig. 10. Notably, the fact that the size-gradation curve for the sorted surface sediment in the straight reach crosses that for the initial bed sediment indicates that proportionally more of the medium-size particles are moved away because some of the finer ones find their ways to hide behind the coarser ones.

Further analysis of sediment samples taken from the outer bank region for all experimental runs reveals that the proportion of particles remained on the sieve of the largest opening increases with increasing P values, as shown in Table 7. This phenomenon is actually coupled with the high proportion of finer particles existing in the inner bank region for runs with higher P values as mentioned earlier.

From Table 8, one can see that the σ/σ_o values at the peak of hydrograph generally increases from inner bank towards outer bank, with the exception that it drops off at $r/r_c = 1.094$, where the side wall effect may be present. This variation may be attributed to the fact that primarily during the rising limb, the medium size particles are transported from the outer bank region. Therefore the σ/σ_o value is substantially larger than 1.0 in the outer region ($r/r_c = 1.056$) and not much smaller than 1.0 in the inner region ($r/r_c = 0.906$);

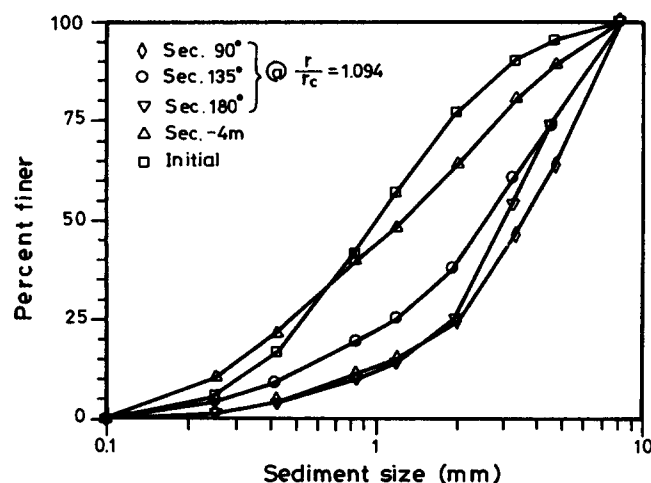


FIG. 10. Sediment-Size Gradation Curves at End of Run 1

TABLE 7. Sediment-Size Fractions (%) for Section 90° at $r/r_c = 1.094$

Size (mm) (1)	Run				
	1 (2)	2 (3)	3 (4)	4 (5)	5 (6)
8.52	36.06	32.77	28.18	25.75	23.92
4.76	17.46	16.33	20.54	16.90	17.13
3.36	21.94	23.30	28.90	24.57	22.05
2.00	9.29	10.82	8.63	10.34	12.52
1.19	3.63	3.21	3.35	4.57	4.56
0.84	7.08	6.10	6.37	9.43	9.63
0.42	3.13	3.47	2.63	5.42	5.58
0.25	1.41	4.00	1.40	3.02	4.61

TABLE 8. Variation of σ/σ_o at Section 90°

Time (1)	Run (2)	r/r_c					
		0.906 (3)	0.944 (4)	0.981 (5)	1.019 (6)	1.056 (7)	1.094 (8)
Peak	1	0.86	0.88	1.08	1.41	1.42	1.37
Peak	2	1.03	1.10	1.18	1.35	1.38	1.34
Peak	3	0.93	1.00	1.13	1.17	1.24	1.18
Peak	4	0.86	0.92	0.99	1.15	1.30	1.21
Peak	5	0.85	1.03	1.18	1.18	1.29	1.20
End	1	0.66	0.64	0.77	0.81	1.00	0.83
End	2	0.91	0.91	0.90	1.07	0.87	0.88
End	3	0.60	0.61	0.96	1.12	0.99	0.88
End	4	0.59	0.76	0.98	1.13	1.08	1.05
End	5	0.64	0.67	0.97	1.06	1.12	1.11

however, it is greater than 1.0 in the central region. Meanwhile, as more sorting action takes place during the recession limb, the σ/σ_o value decreases in all the areas within the bend at the end of the hydrograph. This decrease may be attributed to the fact that as the flow recedes, more of the finer particles are transported from the outer region to the inner region. Therefore, at the end of the hydrograph the σ/σ_o value of the sediment on the bed surface becomes much smaller than 1.0 in the inner region ($r/r_c = 0.906-0.944$), and it is generally close to 1.0 in the outer region ($r/r_c = 1.019-1.056$). This occurrence implies that the sediments are less graded in both regions at the end of the hydrograph compared with those at the peak.

The experiments in this study were done under the conditions having no sediment inflow from upstream and a flat initial bed with uniformly mixed material. This is actually not the case in natural meandering rivers, as Dietrich and Smith (1984) pointed out. Under the conditions of the present experiments, however, the deposition height, scour depth and sorting action should be greater than those in the case having sediment inflow from upstream and initially deformed bed with well sorted material. Therefore, the results presented herein may be regarded as being on the safe side for engineering applications.

Sediment Discharge

As previously mentioned, the total amount of sediment collected in the settling tank at the end of each run increases with a increasing P value. When the total weight is broken down into two parts, i.e., one for the rising limb of the hydrograph and the other for the falling limb, as shown in Table 5, it reveals that the former is less than the latter, except for run 5. This is so because the recession period is twice as long as the rising period. In the case of run 5 with the given flow condition, the proportion of the particles vulnerable to transportation is quite possibly very small to begin with and much less available during the falling limb of the hydrograph. Also, the d/d_o and σ/σ_o values are all less than 1.0, except for one case. This clearly indicates that most of the sediment transported downstream is of medium and finer portions. There is a general trend that σ/σ_o value decreases with a decreasing P value. This may be accounted for by the fact that as P decreases more of the finer particles in proportion are transported downstream and therefore tend to be more uniform.

Although the total flow work index W_f is the same for all five runs, the variation of total amount of sediment transported W_s is quite substantial, thereby reflecting the influence of unsteady flow parameter P . The relation between W_s and P_1 is shown in Fig. 11. A regression analysis for the data shown yields the following:

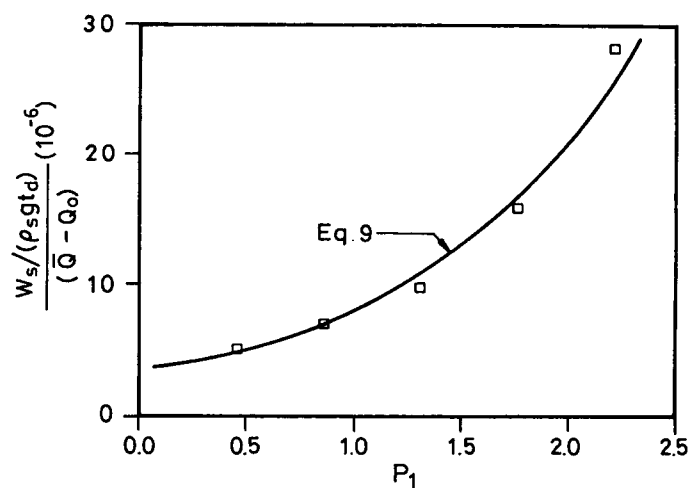


FIG. 11. Sediment Discharge as Function of P_1

$$\frac{W_s}{\rho_s g t_d} = 3.04 \times 10^{-6} \exp(0.97 P_1) \quad (9)$$

where Q_o = the discharge of base flow; and \bar{Q} = the mean discharge of hydrograph. The regression equation may be used for preliminary estimation of the average transport rate during a flood event that has a similar hydrograph shape and is in the same range of P_1 value as those of the present experiments. Further investigations are required to cover other hydrograph characteristics.

CONCLUSIONS

The following conclusions can be made on the basis of this study.

For the present study in the 180° channel bend with a constant radius of curvature, the bed deformation and transverse sorting of sediment become significant beginning around sections 30° and 15°, respectively. Additionally they both gradually reduce after section 180° as the secondary current decays. Experimental results clearly indicate that the unsteady flow parameter P exerts a strong influence on bed deformation and sediment sorting. The scour depth, deposition height, and transverse sorting all increase with increasing P value.

Experimental results also indicate that the maximum deposition height takes place between sections 75° and 90°, and the maximum scour depth occurs between sections 165° and 180°. The transverse bed profiles for the sections with maximum deposition and scour can be approximated by (5), in which coefficients a_1 , b_1 , and c_1 are dependent on parameter P .

The most intensive transverse sorting occurs in the area around section 90°, and the transverse variation of median sediment size for this section can be approximated by (7), in which coefficients a_2 , b_2 , and c_2 are also dependent on parameter P .

The actions of the secondary flow and high velocity in the outer-bank region result in that the bed surface sediments are more uniform both in the inner- and outer-bank regions than that in the central region. Analysis of sediment samples taken from the bed surface also reveals that the uniformity increases with increasing P value.

The total amount of sediment transported during a hydrograph is closely related to P . A regression relation is obtained as given in (9) which may be used for preliminary estimation of sediment transported in flood events having similar characteristics as those in the present experiments.

ACKNOWLEDGMENTS

The experimental facilities provided for the study reported herein, by the Hydraulic Research Laboratory, National Taiwan University, Taipei, Taiwan, is hereby gratefully acknowledged. Financial support by the National Science Council, Taiwan, under grant NSC-79-0410-E002-46 is highly appreciated. Thanks are also due to Tien-pin Liao and Han-feng Chiu for their laborious work in performing experiments.

APPENDIX I. REFERENCES

- Allen, J. R. L. (1970). "A quantitative model of grain size and sedimentary structures in lateral deposits." *Geological J.*, 7, 129–146.
- Bridge, J. S. (1976). "Bed topography and grain size in open channel bends." *Sedimentology*, 23(3), 407–414.
- Dietrich, W. E., and Smith, J. D. (1984). "Bed load in a river meander." *Water Resour. Res.*, 20(10), 1355–1380.
- Engelund, F. (1974). "Flow and bed topography in channel bends." *J. Hydr. Div.*, ASCE, 100(11), 1631–1648.
- Falcon, M. A., and Kennedy, J. F. (1983). "Flow in alluvial-river curves." *J. Fluid Mech.*, 133, 1–16.
- Graf, W. H., and Suszka, L. (1985). "Unsteady flow and its effect on sediment transport." *Proc. 21st Congress*, International Association for Hydraulic Research, Delft, The Netherlands, 540–544.
- Griffiths, G. A., and Sutherland, A. J. (1977). "Bedload transport by translation waves." *J. Hydr. Div.*, ASCE, 103(11), 1279–1291.
- Ho, S. Y. (1987). "Flow characteristics and evolution of bed topography in meandering channels with fixed banks." PhD thesis, National Taiwan University, at Taipei, Taiwan.
- Ikeda, S., Yamasaka, M., and Chiyoda, M. (1987). "Bed topography and sorting in bends." *J. Hydr. Engrg.*, ASCE, 113(2), 190–206.
- Kikkawa, H., Ikeda, S., and Kitagawa, A. (1976). "Flow and bed topography in curved open channels." *J. Hydr. Div.*, ASCE, 102(9), 1327–1342.
- Lee, K. T. (1991). "The effects of unsteady flow characteristics on bed topography and sediment gradation in river bends." PhD thesis, National Taiwan University, at Taipei, Taiwan.
- Little, W. C., and Mayer, P. G. (1972). "The role of sediment gradation on channel armoring." *ERC-0672*, School of Civ. Engrg., Georgia Inst. of Technol., Atlanta, Ga.
- Nouh, M. (1989). "Self armoring process under unsteady flow conditions." *Proc. 23rd Congress*, International Association for Hydraulic Research, Delft, The Netherlands, B49–56.
- Odgaard, A. J. (1982). "Bed characteristics in alluvial channel bends." *J. Hydr. Div.*, ASCE, 108(11), 1268–1281.
- Rozovskii, I. L. (1961). "Flow of water in bends of open channels." *No. OTS 60-51133*, Y. Prushansky, translation, Office of Technical Services, U.S. Dept. of Commerce, Washington, D.C.
- Yen, B. C. (1965). *Characteristics of subcritical flow in a meandering channel*. Iowa Inst. of Hydr. Res., Iowa City, Iowa.
- Yen, C. L. (1967). "Bed configuration and characteristics of subcritical flow in a meandering channel." PhD thesis, University of Iowa, at Iowa City, Iowa.
- Yen, C. L., and Lee, K. T. (1991). "Effects of reservoir on bed topography and sediment gradation of downstream channel bends (III)." *Research Report No. 126*, Hydr. Res. Lab., Nat. Taiwan Univ., Taipei, Taiwan (in Chinese).
- Yen, C. L., and Lin, Y. L. (1990). "Bed material and bed topography in channel bend." *Proc. 7th Asian and Pacific Div. Congress*, International Association for Hydraulic Research, Delft, The Netherlands, 1, 213–218.
- Zimmermann, C., and Kennedy, J. F. (1978). "Transverse bed slopes in curved alluvial streams." *J. Hydr. Div.*, ASCE, 104(1), 33–48.

APPENDIX II. NOTATION

The following symbols are used in this paper:

- a_1, b_1, c_1 = coefficients in (5);
- $a_{1i}, b_{1i}, b_{12}, c_{1i}$ = coefficients in (6), $i = 1, 2, 3, 4$;
- a_2, b_2, c_2 = coefficients in (7);
- B = channel width;
- b_{ns} = coefficient relating τ_{om} to τ_{os} ;
- d = median diameter of sediment;
- $d_{15.9}$ = grain size of 15.9% finer;
- $d_{84.1}$ = grain size of 84.1% finer;
- d_i = mean diameter of i th size fraction of sediment;
- d_o = initial median diameter of sediment;
- F_i = functions, $i = 1, 2, 3, \dots, 6$;
- f = Darcy-Weisbach friction factor;
- g = gravitational acceleration;
- h = flow depth;
- h_u = base flow depth at upstream end;
- h_p = flow depth at peak of hydrograph at upstream end;
- n = transverse coordinate;
- $P = (h_p - h_u)/(t_d u_{*o})$, unsteady-flow parameter;
- $P_1 = P \times 10^4$;
- \bar{Q} = mean discharge of hydrograph;
- Q_o = discharge of base flow;
- r = radial coordinate of channel bend;
- r_c = radius of curvature along central line in bend;
- s = longitudinal coordinate;
- t = time;
- t_d = duration of hydrograph;
- u_{*o} = shear velocity of base flow in upstream straight reach;
- W_s = total weight of sediment transported during t_d ;
- W_t = index of total flow work;
- Z_b = bed-surface elevation;
- α = shape factor of sediment particle;
- $\beta = (\rho_s - \rho)/\rho$;
- ΔZ_b = change in bed-surface elevation;
- δ_i = deviation angle of path of sediment particle having size d_i ;
- θ = angular coordinate of bend;
- θ_s, θ_n = longitudinal and transverse bed slopes, respectively;
- λ = sheltering coefficient of sediment;
- ρ = density of water;
- ρ_s = density of sediment particle;
- σ = standard deviation of sediment-size gradation;
- σ_o = standard deviation of initial sediment-size gradation;
- τ_{om}, τ_{os} = the n - and s -components of the bed shear stress, respectively; and
- ∇ = total volume of water under the hydrograph, excluding base flow.